Articles in PresS. Physiol Genomics (August 1, 2006). doi:10.1152/physiolgenomics.00084.2006

Coordinated multi-tissue transcriptional and plasma metabonomic profiles following acute caloric restriction in mice.

[φ]Colin Selman[§Δ], Nicola D. Kerrison[*Δ], Anisha Cooray[ψ], Matthew D.W. Piper[‡], Steven J. Lingard[§], Richard H. Barton[ψ], Eugene F. Schuster*, Eric Blanc*, David Gems[‡], Jeremy K. Nicholson[ψ], Janet M. Thornton[*], Linda Partridge[‡], Dominic J. Withers[§]

*[§]Centre for Diabetes and Endocrinology, Department of Medicine, University College London, Rayne Institute, 5 University Street, London WC1E 6JJ, UK; *EMBL - European Bioinformatics Institute, Wellcome Trust Genome Campus, Hinxton, Cambridge, CB10 1SD, UK; [ψ]Biological Chemistry Section, Department of Biomolecular Medicine, SORA Division Faculty of Medicine, SAF Building, Imperial College London, South Kensington, London, SW7 2AZ, UK; [‡]UCL Centre for Ageing Research, Department of Biology, University College London, Darwin Building, Gower Street, London WC1E 6BT, UK.*

[Δ]Both authors contributed equally to this manuscript

[φ]Address correspondence to:
Colin Selman, Centre for Diabetes and Endocrinology, Department of Medicine, University College London, Rayne Institute, 5 University Street, London WC1E 6JJ, UK.
e-mail: c.selman@ucl.ac.uk
phone +442076796588 fax +442076796583

Running Head: Multi-tissue transcriptional and metabolite response to acute caloric restriction

ABSTRACT

Caloric restriction (CR) increases healthy lifespan in a range of organisms. The underlying mechanisms are not understood, but appear to include changes in gene expression, protein function and metabolism. Recent studies demonstrate that acute CR alters mortality rates within days in flies. Multi-tissue transcriptional changes and concomitant metabolic responses to acute CR have not been described. We generated whole-genome RNA transcript profiles in liver, skeletal muscle, colon and hypothalamus and simultaneously measured plasma metabolites using proton nuclear magnetic resonance in mice subjected to acute CR. Liver and muscle showed increased gene expression associated with fatty acid metabolism and a reduction in those involved in hepatic lipid biosynthesis. Glucogenic amino acids increased in plasma and gene expression for hepatic gluconeogenesis was enhanced. Increased expression of genes for hormone-mediated signaling and decreased expression of genes involved in protein binding and development occurred in hypothalamus. Cell proliferation genes were decreased and cellular transport increased in colon. Acute CR captured many, but not all, hepatic transcriptional changes of long-term CR. Our findings demonstrate a clear transcriptional response across multiple tissues during acute CR, with congruent plasma metabolite changes. Liver and muscle switched gene expression away from energetically expensive biosynthetic processes towards energy conservation and utilization processes, including fatty acid metabolism and gluconeogenesis. Both muscle and colon switched gene expression away from cellular proliferation. Mice undergoing acute CR rapidly adopt many transcriptional and metabolic changes of long-term CR, suggesting that the beneficial effects of CR may require only a short-term reduction in caloric intake.

Key Words: Caloric restriction, Aging, Microarray, Metabolite, Gene expression

INTRODUCTION

Caloric restriction (CR) extends mean and maximum lifespan and retards various age-associated pathologies in a range of vertebrate and invertebrate species (24, 41, 46, 61). However, the mechanisms through which CR extends lifespan are not understood. CR is accompanied by changes in gene and protein expression and resultant alterations in both cellular and whole organism metabolism, which are thought to underlie its effects on ageing.

RNA transcript profiles have been useful for defining changes in gene expression following CR, leading to the formulation of experimentally testable hypotheses. Long-term CR in rodents attenuates many age-associated transcriptional changes, including expression of genes involved with cellular stress, in skeletal muscle (36), hypothalamus (20) and liver (11, 16). However, to date, most microarray mRNA expression studies in mice have been confined to single tissues and have profiled only part of the genome. In addition, single-tissue studies have varied widely both in experimental design, bioinformatic analysis and in the mouse strains used (29), thus making direct comparisons between tissues difficult. Furthermore, altered transcript profiles have not been related to concomitant plasma metabolic changes.

Changes in gene expression following initiation of CR (or dietary restriction, DR) appear rapid in both *Drosophila* and mice. Significant shifts in transcript profile in *Drosophila* occurred within 3 days following DR (47). In studies of hepatic gene expression in mice, a rapid and cumulative shift mirroring a long-term (12-month) CR transcriptional profile was observed following 2, 4 or 8 weeks of CR. A return to *ad*

libitum (AD) levels reversed 90% of this long-term CR profile after 8 weeks (16). This suggests that these changes in gene expression during acute CR may induce rapid beneficial effects on lifespan. In *Drosophila*, a dietary shift to DR altered mortality rate within days (40). However, accurate measurements of mortality rates during acute CR have not been measured in mice, although CR initiated at 12 months of age extended mean and maximum lifespan, decreased age-associated mortality and reduced cancer incidence (16, 49).

In this study we examined acute, whole-genome transcriptional changes following short-term CR, in liver, skeletal muscle, hypothalamus and colon of 16 week old male C57BL/6 mice subjected to a stepwise, 16-day protocol of CR terminating in a 48h period of 30% CR (see supplementary data). In parallel, we employed a NMR metabonomic strategy capable of identifying subtle biochemical changes (56) to determine plasma metabolite profiles during CR in the same animals subjected to transcriptional analysis, as plasma should relate directly to global metabolic changes in the concentration of metabolites. Our experimental design therefore permitted simultaneous examination of tissue-specific and common changes in gene expression together with relevant metabolic end-points.

We show that both liver and muscle switch away from energetically expensive biosynthetic processes towards fatty acid metabolism, β-oxidation and gluconeogenesis as the dominant energy pathways during acute CR. This enhanced gluconeogenesis appears fuelled by skeletal muscle (and perhaps colon) catabolism, with genes associated with growth down-regulated in both tissues, and an associated increase in plasma of

several glucogenic amino acids. A simultaneous decrease in plasma levels of glucose and several lipids was also observed.

METHODS

Study design. 20 male C57BL/6 mice were purchased from a commercial breeder (Harlan, U.K.) at 4 weeks of age and housed at ~22°C under a 12h light/dark cycle (lights on from 0700 to 1900 h; Imperial College, London, UK). Mice were maintained in groups of 5 (see (28)) under specific pathogen-free conditions within individually ventilated cages (Techniplast U.K. Ltd, U.K.), with *ad libitum* (AD) access to normal chow (2018 Teklad Global 18% Protein Rodent Diet, Harlan Teklad, U.K.) and water. The manufacturers (Harlan Teklad, U.K.) report that proximate analysis of the chow diet consisted of crude protein (18.90%), crude oil (5.70%), crude fiber (3.80%), ash (5.90%), NFE (55.70%), carbohydrate (57.33%), starch (41.24%), sugar (4.93%), plus pre-defined minerals, amino acids, vitamins and fatty acids. The main saturated, mono-unsaturated and polyunsaturated fatty acid components (g/kg diet) of the diet were respectively, palmitic acid C16:0 (7.64g/kg), oleic acid C18:1w9 (12.59g/kg) and linoleic acid C18:2w6 (31.35g/kg). The total levels of digestible and metabolizable energy in the diet were 3.4Kcal/g and 3.3Kcal/g respectively. At 12 weeks of age, mice in different cages did not significantly differ from one another in body mass, and each cage was randomly assigned to the CR or AD feeding regime. The experiment commenced at 14 weeks of age, with the time of feeding of the CR mice being 0900 each day, in agreement with feeding time in other studies, e.g. (16). Food was not removed from either the CR or the AD mice at any time during the day, with the hoppers of the CR mice always being empty by 0900hrs of the following day. Food intake of CR mice was adjusted according

to the intake of AD mice measured the preceding week. CR mice underwent a step-down regime (see supplementary data) similar to protocols described elsewhere (43), with daily food intake reduced to 90% of AD mice at 14 weeks, 80% at 15 weeks and 70% at 16 weeks of age, *i.e*. 30% CR relative to AD controls. CR mice were not fed in the morning immediately prior to death. Neither group underwent a 24 h (16) or 48 h (11) fast prior to death, as we wished to avoid inducing acute starvation conditions that may transcriptionally mirror those seen during CR (8). Exactly 48 h after the initiation of 30% CR, 10 mice per group (CR or AD) were killed by terminal anesthesia (IP injection of fentanyl/fluanisone (Hypnorm; Janssen Animal Health, U.K.) and benzodiazepine mix (Midazolam; Roche, U.K.) between 0900-1200h. Individuals in each group were killed alternately to minimize any circadian effects, and the left lobe of liver, the gastrocnemius, hypothalamus (block containing dorsomedial, ventromedial, arcuate and paraventricular hypothalamus) and a 2cm portion of the upper colon were removed, flash-frozen in liquid nitrogen and stored at -80°C until RNA extraction. In order to minimize the potential for hierarchies to develop within our group-housed mice, we purchased mice that had been weaned together from 4 weeks of age. These same individuals were then maintained in groups of five individuals until death. In addition, all large food pellets were broken into smaller pieces to further avoid the potential for any one individual to monopolize the food supply. We observed no evidence of hierarchies in our group-housed CR or AD mice, either in terms of body mass differences within cages or in terms of fighting. All mice were monitored daily, and in agreement with Ikeno et al. (28) all CR mice were able to feed simultaneously at the hopper with no evidence that any one individual interfered with the feeding behaviour of any other mouse within a cage. No signs of pathology were

observed in any mice and all procedures followed local ethical and UK Home Office guidelines.

*Tissue preparation for DNA microarray analysis***.** Individual samples were pooled in triplicate (individuals AD or CR 1-3, 4-6, 7-9) prior to RNA extraction with the remaining sample (AD 10 or CR 10) equally distributed between each of the three groups, with ~100mg (Ohaus U.K. Ltd, U.K., 0.0001g) of tissue taken from each individual. The hypothalamus weighed ~100mg, therefore samples from individual AD10/CR10 were divided equally between the three pooled groups. Several recent studies suggest that pooling individual samples gives an accurate measure of the average expression (30, 31). The pooling strategy adopted was partially based on the methods suggested by Kendziorski et al. (30), and employed to help reduce the effects of biological variability, i.e. maximize our ability to detect the effects of experimental treatment. Samples were prepared according to Affymetrix protocols (Affymetrix U.K. Ltd, www.affymetrix.com). In brief, samples were homogenized on ice using a Positron homogenizer in TRIzol reagent (Invitrogen Corp, U.K.), followed by purification using RNeasy columns (Qiagen Ltd, U.K., www1.qiagen.com), with RNA quality and concentration determined using an Agilent Bioanalyzer 2100 (Agilent Technologies, CA, US).

Microarray measurement of gene expression. Changes in transcript abundance were measured using mouse whole-genome oligonucleotide microarrays (Mouse Genome 430 2.0 Array, Affymetrix), with all protocols undertaken at the Institute of Child Health (ICH) Gene Microarray Centre, University College London, U.K. 3 biological replicates were analyzed for each condition (acute CR or AD control). The cRNA probe generation,

washing, labeling and scanning followed Affymetrix and ICH Gene Microarray Centre standard protocols.

Statistical analysis of transcript representation. Raw image files were converted to probe-level data files (.cel files). Normalization, statistical testing and multiple testing correction of data files used the R (www.R-project.org) package Goldenspike (13). A false discovery rate cut-off of 0.05 was used to generate lists of genes whose expression was significantly altered by CR for all tissues except colon, as a q-value cutoff of 0.05 resulted in only 22 up- and 11 down-regulated probesets. Because changes in the colon were more subtle than in other tissues, the stringency was lowered to reflect this. We chose the value of 0.11, an optimal point in the sense of maximizing the gene list length while keeping the q value cutoff as low as possible. Probes were mapped to transcript sequences from the Ensembl mouse genome (Version 27.33c.1). Acceptable matches were defined as having at least 7 of the 11 probes in the probe set matching the gene transcript with no more than 2 mismatches, and no other gene matched by more than three probes in the probe set. This procedure mapped approximately 47% of the probe sets on the mouse genome 430 2.0 array. Gene Ontology (Gene Ontology Consortium), Interpro and Locuslink annotation for the genes was retrieved from Ensembl. Kegg annotation was mapped to genes via Locuslink identifiers. These annotations, together with EASE (Expression Analysis Systematic Explorer (25)) were used to identify over-represented annotation categories within the gene lists, scored using the EASE score, and significance calculated using a modified Fisher's Exact Test. For analyses not involving EASE, unmapped probe sets were annotated with information from Affymetrix's NetAffx site (39). In our EASE comparison with the long-term CR data set (16), we reported those

genes which mapped directly to Ensemble gene lists. Raw microarray data is available in the European Bioinformatics Institute (EMBL-EBI) ArrayExpress repository (Accession Number E-MEXP-748).

In our tissue-comparative approach, we recorded the number of differentially expressed probe sets in each tissue, and the number of probe sets differentially expressed in several tissues. The significance of overlaps between tissues in probe sets differentially expressed during CR was tested with the null hypothesis that each probe was randomly and independently selected from the pool of all probe sets represented on the microarray. Using Fisher's Exact Test, we calculated the probability of an overlap occurring by chance. The probabilities calculated must be treated with some caution because in reality genes are not randomly and independently expressed. However, these probabilities provide an indication of similarities between tissues' responses to CR. We examined overlaps of EASE-generated lists over-represented ($p<0.1$) from the differentially expressed probe sets. Probability estimates were adjusted for multiple testing using a Bonferroni Correction, with adjusted scores $p< 0.05$ deemed significant.

Metabonomic sample preparation, ^{1}H nuclear magnetic resonance (NMR) spectroscopy and multivariate data analysis. Blood was collected under terminal anesthesia by cardiac puncture, centrifuged (8000 rpm for 15 min at 4°C), and the resulting plasma stored at -80°C until analysis. 200µl aliquots of each sample were transferred into 5mm NMR tubes and diluted with 300µl extender solution, comprising isotonic saline (0.9 % w/v), 3mM Sodium azide and 20% v/v D_2O. ^{1}H NMR spectroscopy and data reduction are described in detail elsewhere (9). All resulting ^{1}H NMR spectra were manually phased, baseline corrected using XWINNMR software (Bruker Biospin Ltd, U.K.) and the glucose

anomeric proton signal at 5.23 ppm used as a frequency reference to calibrate the position of spectra. Subsequent automatic data reduction and normalization to unit total for each spectral integral was then carried out (9), and the reduced and normalized NMR spectral data were exported to SIMCA-P (Version 10.5, Umetrics AB, Umeä, Sweden) and mean-centered without further scaling. ^{1}H NMR spectroscopy generates large datasets containing a range of metabolic information, so to extract meaningful and clear information related to pathophysiological stimuli, datasets were simplified using principal component analysis (PCA (63)) and partial least squares (PLS (64)) methods. It is important to note that this data reports concentrations of metabolites in plasma and does not represent measurements of metabolic flux.

Microarray data validation by real-time PCR. Real-time PCR was performed as previously described (14). TaqMan® gene expression assays (Symbol, Assay ID) for Forkhead box 01/Forkhead transcription factor 1

(Foxo1, Mm00490672_m1), Peroxisome proliferator activated receptor alpha (Ppara, Mm00440939_m1), DNA-damage-inducible transcript 4 (Ddit4, Mm00512503_g1), Diacylglycerol O-acyltransferase 2 (Dgat2, Mm00499530_m1) and Insulin receptor substrate 1 (Irs1, Mm00439720_s1) were run in duplicate. Transcription elongation factor A (SII) 1 (Tcea1, Mm00815387_s1) was amplified as a control, as its expression was unaffected by CR in both this study and in others, e.g. (16). We tested 3 pooled liver samples, as described earlier, in both CR and AD mice and a further 20 unpooled samples consisting of the 10 individual mice per group (CR1:10 and AD1:10) from which our pools were derived. We employed the comparative C_T method, with fold-changes

calculated according to expression; $2\text{-}\Delta\Delta C_T$. P values refer to a one-tailed t-test between normalized C_T values (C_T target gene – C_T Tcea1) of CR vs. AD mice(1) .

RESULTS

Acute CR reduced body mass. CR mice showed a 12% reduction in body mass (Mean±SEM; CR 26.5±0.6g, control 30.0±0.6g, F=16.2, P<0.01) compared to AD mice. Body mass during the experiment (final body mass - initial body mass prior to CR) increased in AD mice by 1.1±0.3g and decreased in CR mice by 1.4±0.2g. Every single mouse in the CR group (n=10) decreased in body mass during the period of CR. One mouse from the AD group (n=10) decreased in mass (-0.4g) during this same period of time.

Acute CR altered plasma metabolite profile. NMR spectroscopy clearly distinguished the plasma metabolite profiles of acute CR and AD control mice (Figure 1; Table 1). The Euclidean sum of principal components 1 and 3 in Table 1 indicates the direction and relative change in plasma metabolites between the CR and AD groups, as seen by the position of chemical shift variables in the partial least squares discriminant analysis loadings scatter plot. These results indicate increases in plasma lactate, 3-hydroxybutyrate, cholesterol and associated low density lipoprotein levels under acute CR, in addition to increased plasma creatine and several glucogenic amino acids (methionine, glutamine, alanine, valine), suggesting a metabolic switch towards energy conservation and gluconeogenesis. In agreement, plasma concentrations of glucose and choline were decreased during acute CR, as were the resonances of lipids including very low density lipoproteins (VLDL; 1.25-1.29ppm). The results indicate that the magnitude of change in some plasma metabolites is greater than others. For example, relative to AD

controls, the increase observed in plasma levels of lactate in CR mice is greater than the increase in plasma alanine (Table 1).

Acute CR significantly altered transcript profiles in individual tissues. A total of 1960 probe sets (see supplementary data) showed significantly altered expression in liver (987 higher and 973 lower in CR relative to AD controls; respectively), 520 (213 higher and 307 lower) in skeletal muscle, 309 (152 higher and 157 lower) in colon, and 145 (64 higher and 81 lower) in the hypothalamus. The biological relevance of these changes was assigned using Expression Analysis Systematic Explorer (EASE) analysis (see Table 2, Figure 3 for summary and supplementary data).

Acute CR effects on liver: A metabolic switch towards gluconeogenesis, β-oxidation, and fatty acid metabolism and away from lipogenesis occurred in the liver (Table 2; Figure 2). During acute CR, genes involved in macromolecular biosynthetic processes, such as steroid, sterol and cholesterol biosynthesis, but also amino acid, amino acid derivative and amine metabolism were down-regulated. EASE categories in the up-regulated list included lipid metabolism, palmitoyl-CoA hydrolase activity and acyl-CoA metabolism, with genes identified including Mte1, Cte1, Acadl (initiating gene of β-oxidation), Ppara (Ppar-α) and Hnf-4α. Pgc-1α expression was up-regulated during acute CR, and this protein plays a key role in gluconeogenesis and β-oxidation, co-activates Ppar-α and Hnf-4α, and induces lipolysis. Pgc-1α also modulates energetically expensive biological processes, such as hepatic gluconeogenesis by stimulating mitochondrial biogenesis and oxidative metabolism. This enhancement of mitochondrial biogenesis and oxidative metabolism was further suggested by the identification of the EASE category mitochondrion, which included the genes succinate dehydrogenase (complex II),

cytochrome-c oxidase (Complex IV), several ATP synthases, carnitine carrier/transporter proteins and the mitochondrial transcription factor Tfam.

Acute CR effects on skeletal muscle: A reduction in expression of genes involved in muscle growth and an increase in those involved in fatty acid metabolism occurred in skeletal muscle following acute CR (Table 2; Figure 2). Down-regulated EASE classes included genes associated with protein metabolism, protein transport, cell growth regulation, blood vessel development, collagen and macromolecule biosynthesis. In the up-regulated gene list, EASE categories involved in energy metabolism; including carbohydrate metabolism, carboxylic acid metabolism and fatty acid metabolism were identified. Gene classes involved in MAPK signaling and the JNK pathway were up-regulated, and these are important in growth and development.

Acute CR effects on colon: A decreased expression of genes associated with cellular proliferation but an increase in cellular transport genes was observed in colon following acute CR (Table 2; Figure 2). EASE categories associated with cell growth, cell maintenance and proliferation were down-regulated in the colon following acute CR, including several cyclin-dependent protein serine kinases and serine/threonine protein kinases implicated in tumor formation. In the up-regulated gene list, EASE categories ion transport, rhythmic behaviour and nitric oxide mediated signal transduction were identified. The category transport/ion transport, which included the intestinal-specific epithelial glucose transporter Glut5 (Slc2a5) and Klf15, suggesting transport of metabolic intermediates is enhanced in the colon during acute CR.

Acute CR effects on hypothalamus: In the hypothalamus relatively few EASE categories were identified as being significantly altered following acute CR (Table 2; Figure 2). The

gene category development was identified from our down-regulated gene list, and included the genes Ccnd2 (Cyclin D2), and the forkhead related brain factor Bf-1. Dgkz (Diacylglycerol kinase, zeta) expression was also down, and may play a role in mTOR signaling via phosphatidic acid production, which subsequently induces p70S6K phosphorylation. The category binding was also identified, with several genes involved in protein and calcium binding down-regulated. In the up-regulated gene list, four significant over-represented categories; hormone-mediated signaling, Zn-finger, basement membrane processes and binding, in particular nucleic acid binding.

Significant EASE categorical overlap across tissues in response to acute CR. We tested significance of tissue overlaps between our differentially expressed probe set lists using Fisher's Exact Test. Clear biological similarities in our up-regulated (up in CR) probe set lists were identified (Figure 3), with significant overlap between liver, colon and muscle, and between hypothalamus and liver. In down-regulated probe set lists, liver, colon and hypothalamus showed significant overlap with one another, with muscle showing overlap only with colon. The greatest overlap (50) in probesets was between the down-regulated muscle and the up-regulated liver probe-set list. Three significant EASE categories, containing two genes in each, were identified as up-regulated in liver and down-regulated in muscle, including a protein carrier EASE category (NM_026775, NM_028876). The EASE category 14-3-3 protein contained the genes Ywhae and Ywhag. Ywhae increases resistance to apoptosis via Bcl-2 inhibition, with decreased resistance to apoptosis potentially being important in muscle catabolism observed during CR. The final significant EASE category was ubiquitin-activating enzyme repeat, containing Ube1c (Nedd8 activating) and Uble1b (Sumo-1 activating). Ube1c inhibits steroid receptor-

induced transcription, with hepatic steroid biosynthesis decreased during acute CR. Both are important in cell cycle progression and morphogenesis, possibly explaining decreased expression in muscle during acute CR.

No shared EASE categories were identified across the four tissues in our down-regulated gene lists. However, several were identified in our up-regulated gene lists (Table 3), including transporter activity, ion homeostasis, amino-transferase and zinc ion homeostasis/nitric oxide mediated signal transduction shared across liver and colon. A simultaneous and enhanced requirement for fatty acid metabolism was seen in liver and muscle, with categories including acyl-CoA metabolism, acyl-CoA thioesterase activity and palmitoyl-CoA hydrolase activity (Table 3) identified following acute CR. Our findings demonstrate that shared and common transcriptional responses occur across tissues following acute CR, particularly between liver and colon, and between liver and muscle.

Overlap between tissues in gene expression in response to acute CR. 50 genes were significantly down-regulated in two or more tissues (see supplementary data) following acute CR. Several genes involved in chaperone activity/stress response were down-regulated in two or more tissues, particularly in colon and liver, as were several immune response genes. 79 genes were up-regulated following acute CR across two or more tissues, although none were up-regulated across all four tissues (see supplementary data), with the majority shared between colon and liver (30) or muscle and liver (27).

Similar transcriptional effects of acute and long-term (27 month) CR. We compared our acute hepatic transcriptional data with long-term CR hepatic data derived from 24-hr fasted male B6C3F1 mice, which were group housed, maintained on a defined diet and

undergoing a long-term (27 month) 44% decrease in caloric intake (16). Significant overlap in EASE categories (Figure 4) between acute and long-term CR was observed, with the likelihood of overlaps occurring by chance (Fisher's Exact Probability Test) being $3x10^{-19}$ for the up-regulated and $8x10^{-9}$ for the down-regulated gene categories. 11 out of 46 significant EASE categories identified and down-regulated by long-term CR were shared with acute CR, including lipid metabolism, endoplasmic reticulum and cytochrome P450 (E-class Group I and IV). In the up-regulated gene lists, 20 EASE categories out of 42 significantly over-represented in long-term CR were shared with acute CR, including mitochondrion, electron transport, carboxylic acid metabolism and fatty acid metabolism.

EASE classes identified following long-term CR only. 22 EASE categories were over-represented and up-regulated following long-term CR but not during acute CR, including amino acid catabolism, aromatic compound catabolism, L-phenylalanine metabolism, L-phenylalanine catabolism and oxidoreductase activity. 35 categories were down-regulated following long-term but not short-term CR, including biosynthesis of secondary metabolites, proteasome alpha-subunit, lipocalin-related protein, odorant and pheromone binding.

EASE classes identified following acute CR only. EASE categories changing under acute CR, but not long-term CR, were more numerous with 97 down-regulated and 128 up-regulated. Down-regulated categories included lipid biosynthesis, glutathione S-transferase (Mu class), tRNA metabolism and tRNA ligase activity and up-regulated categories included cell/ion homeostasis, glycerol/triacylglycerol metabolism, acyl-CoA metabolism, fatty acid β-oxidation and rhythmic behaviour.

Discordant effects of long-term and acute CR on EASE classes. Categories for short-chain dehydrogenase/reductase, glucose/ribitol dehydrogenase and B-class cytochrome P450 were up-regulated during acute CR but down-regulated during long-term CR, including B-class cytochrome P450s and short-chain dehydrogenases/reductases. Gene categories associated with amino acid, aromatic compound and amine metabolism showed up-regulation following long-term CR but down-regulation following acute CR.

Validation of microarray results by real-time PCR (RT-PCR). RT-PCR, using five individual genes, was used to independently verify some of our microarray results, in each of the three pooled liver samples derived from our CR and AD mice. All genes reliably produced significant ($P<=0.05$) expression changes (Table 5), with a strong correlation ($r^2=0.982$, $P<0.01$) between fold-changes generated by our microarray and RT-PCR analyses. RT-PCR run on the 20 individual liver samples (AD1:10, CR1:10) from which we derived our RNA pools and using the same five genes showed close agreement between the pooled and unpooled liver RT-PCR and microarray data (Table 5 and supplementary data).

DISCUSSION

Our main findings demonstrating transcriptional responses across multiple tissues, with congruent plasma metabolite changes during acute CR are summarized in Table 5. While changes in RNA transcript abundance will not always be associated with a corresponding change in protein abundance or activity, we suggest that systematic changes in expression of genes involved in the same EASE category imply the presence of a functional change. In addition, it is feasible that some of the genes and pathways reported may be regulated

specifically by CR and AD in C57BL/6 mice, since it appears that '*genotype-regulated genes*' exist between different strains of mice that may affect their response to CR (29).

Acute CR switched gene expression away from lipid biosynthesis and towards fatty acid metabolism and gluconeogenesis. In both the liver and muscle, we saw a simultaneous metabolic shift in transcription towards fatty acid catabolism, β-oxidation and gluconeogenesis, and away from lipid biosynthetic processes. Decreased hepatic lipid biosynthetic gene expression was observed following acute CR. Similar reductions in expression of lipid biosynthetic genes, particularly cholesterol biosynthesis, have also previously been described in long-lived Snell dwarf mice (10). Long-term CR reduces the plasma levels of total cholesterol and plasma triglycerides (18, 37). Our metabonomic analysis indicates this decreased lipid biosynthesis gene transcription coincides with a reduction in several plasma lipid metabolites. Our data indicate that the improved lipid profiles seen following long-term CR and associated with various health benefits (18), occur rapidly upon acute CR, suggesting that even short-term reductions in calorie intake may be beneficial to health. However, plasma cholesterol and associated low density lipoprotein metabolite levels were increased by acute CR, despite a clear reduction in cholesterol biosynthetic gene expression and in contrast to longer-term CR (37). This apparent paradox of high plasma cholesterol but reduced biosynthesis, particularly in liver, may result from transient cholesterol mobilization from white adipose tissue following initiation of CR. These observations suggest that the low plasma cholesterol seen in long-term CR, but not acute CR, is the net result of significantly reduced but steady-state adipose depots and reduced biosynthesis. Enhanced fatty acid metabolism in liver and muscle, in association with reduced plasma glucose, may help explain the

elevated plasma levels of 3-hydroxybutyrate during acute CR. The elevated levels of this ketone body during acute CR suggests an additional requirement for gluconeogenesis to produce C_6 components, when C_4 substrates required for the TCA cycle (e.g. oxaloacetate) may be in deficit.

Enhanced hepatic mitochondrial gene expression following acute CR. Genes involved with electron transport and EASE classes linked to mitochondrial function were up-regulated in the liver. We suggest that shifts in cellular metabolic pathways observed during acute CR, such as gluconeogenesis and β-oxidation, are energetically expensive and require enhanced mitochondrial function to provide ATP. It has recently been shown that CR (3 or 12 months duration) promotes mitochondrial biogenesis in several tissues via endothelial nitric oxide synthase (eNOS) induction, leading to elevated oxygen consumption, increased mitochondrial DNA levels (marker of mitochondrial content) and ATP production (45). While, no significant expression changes in any isoform of NOS was observed, several genes central to mitochondrial biogenesis and function, including Pgc-1α, Tfam, and cytochrome c (Cycs), were significantly up-regulated in liver following acute CR.

Acute CR increased protein catabolism in skeletal muscle. EASE categories linked to ubiquitination, protein targeting and transport, collagen deposition, blood vessel development and cell growth were all down in muscle during acute CR. Lean body mass, which includes muscle mass, is lost rapidly in humans under acute CR (19) and muscle mass in rats subjected to 8 weeks of 40% CR was significantly reduced (54). The elevation of the branched amino acid valine in plasma in our study is consistent with increased muscle turnover. Muscle catabolism during CR may provide gluconeogenic

precursors (57). Gpt2 and Tkt, involved in carbon metabolism, and glutamine synthase (Glul) which is important in disposal of the products of protein catabolism, were all up-regulated in muscle. Elevated plasma levels of the glucogenic amino acids methionine, valine, glutamine and alanine and also creatine were seen in acute CR mice, consistent with enhanced gluconeogenesis. In addition, the elevated plasma levels of lactate and alanine suggest that glucose-utilizing tissues may only partially catabolise glucose, thus sparing carbon skeletons which can then fuel hepatic gluconeogenesis. We suggest that increased requirement for hepatic gluconeogenesis, in conjunction with muscle catabolism, during acute CR may help explain the elevated plasma methionine levels observed.

Altered transcript profile relevant to insulin sensitivity during acute CR. Both long-term (3) and short-term CR improve insulin sensitivity in muscle (12) and decrease both plasma insulin and glucose (2, 4, 22), which may play a key role in lifespan extension (20). We saw reduced plasma glucose in mice following acute CR, and up-regulation of glucose homeostatic genes, including Pgc-1α, Ppar-α, Hnf-4α and Foxo1, particularly in liver and muscle. Several genes implicated in insulin resistance were down-regulated, particularly in muscle, including protein kinase C activator Cish, protein kinase C substrate Marcks and Socs3. In the hypothalamus, the receptor for adiponectin (Adipor2), which promotes insulin sensitivity, was up-regulated. The observed increase in plasma lactate following acute CR appears counter-intuitive, but may be associated with the reduced plasma glucose observed at this time. Lactate production is not only a consequence of anaerobic metabolism in contracting skeletal muscle, but is formed continuously under aerobic conditions and is, as mentioned previously, an important C_3

metabolite produced in the brain and utilized during hepatic gluconeogenesis in periods of reduced energy availability. Lactate uptake in mitochondria and pyruvate-lactate release in peroxisomes is important in re-oxidation of NADH, anaplerotic reactions, and is essential to both gluconeogenesis and β-oxidation, both of which appear transcriptionally up-regulated by acute CR in liver and muscle.

Alterations in energy balance during acute CR. The colon and hypothalamus are crucial to energy balance, playing key roles in energy assimilation and energy sensing, and the regulation of food intake and energy expenditure, respectively (6). These tissues are likely to be vital for successful adaptation to CR. In contrast to longer-term CR (20), we observed increased hypothalamic pro-MCH precursor (pro-melanin-concentrating-hormone) and orexin precursor gene expression, suggesting that there is a drive for enhanced food intake during acute CR. In contrast to Fu et al. (20), we saw no down-regulation of stress response, protein folding or heat response EASE categories (20), although Hspa1b and Hspb1 were down-regulated. In the colon, we saw down-regulation of genes involved in cellular proliferation and maintenance. These transcriptional changes may contribute to the reduced incidence of colon cancer seen during long-term CR (51), and may also reflect an acute energy saving mechanism or reduced nutrient transit through the gut at this time. The colon could also act as an additional energy source for hepatic gluconeogenesis. Up-regulation of genes involved in cellular transport was observed and may improve extraction and utilization of available energy from the diet, which may be vital to successful adaptation to CR.

Potential longevity assurance genes identified during acute CR and associated with insulin/insulin-like growth factor signaling. Considerable recent interest has focused on

mutations in insulin/insulin-like growth factor signaling (IIS), and on how CR and aging impinge on this pathway (32, 41). Both treatments ultimately encroach on nutrient sensing. An elegant study comparing CR and Ames mice indicated that both groups shared an overlapping group of genes, but also both treatments additively affected a panel of genes, suggesting some shared transcriptional responses (58). Our cross-tissue comparison revealed several IIS pathway genes, particularly in liver and muscle, differentially expressed following acute CR. Expression of insulin-receptor substrate protein 1 (Irs1) was down-regulated in both liver and muscle following acute CR. Short-term CR (20 days) reduced IRS1 protein expression (22) in mouse skeletal muscle. However, during longer-term CR (14-months), basal tyrosine phosphorylated IRS1 protein levels in mouse skeletal muscle appeared unchanged (2, 3), although a non-significant trend to increase (~170%) was reported (3). IRS1 knockout mice share some phenotypic similarities with long-lived dwarf mice (7, 62) and lifespan in *chico* (dIRS) null flies is enhanced (15).

The forkhead transcription factor Foxo1 (Fkhr) was up-regulated in both liver and muscle following acute CR, as was Foxo3a (Fkhrl1) in the liver. The lifespan extension in daf-2 *C. elegans* mutants requires daf-16 (Foxo) activity (38), although it appears non-essential for the lifespan effects of DR (26, 35). Over-expression of dFoxo in the adult *Drosophila* fat body, increased life-span and reduced fecundity in female flies (23, 27). Foxo1 also appears to regulate various stress response genes in mammals, including Gadd45, which was also up-regulated in liver and muscle (34). In addition, Ppar-α, up-regulated in the liver (and colon), is a powerful co-regulator of Foxo1 and both appears central to *de novo* glucose synthesis (50).

The expression of Redd1 (Ddit4/Rtp801), a hypoxia-inducible factor responsive gene, was enhanced in liver and muscle. The Drosophila Redd1 paralogs *Scylla* and *Charybdis* are stress-induced negative regulators of growth and appear critical for survival under hypoxia and low nutrient conditions (52). Over-expression of these paralogs down-regulates S6 kinase signaling via the target of rapamycin (TOR) signaling pathway (52). Interestingly, global deletion of S6K1 in mice causes mild growth retardation, enhanced insulin sensitivity and reduced fat mass (60), all features shared by CR rodents and to an extent by Ames dwarf mice (17). In addition, the translational repressor 4e-bp1 (Eif4ebp1) was up-regulated in both liver and muscle following acute CR, with an increase in protein levels of 4E-BP1 reported in the liver of Ames mice compared to control mice (55).

Potential longevity assurance genes identified during acute CR and associated with circadian rhythm. Circadian rhythm influences many physiological activities, including sleep-wake cycles, endocrine function, body temperature, hepatic metabolism and detoxification (53). Several period circadian transcriptional factors (Per1, Per2, Per3, Usp2) were up-regulated in liver, muscle and colon following acute CR, as were associated circadian proline- and acid-rich (PAR) basic leucine zipper (bZip) transcription factors (Dbp, Hlf, Tef) in the liver. Arntl/Bmal1 was down-regulated in liver, muscle and colon. Mice with combined deletion of Dpb, Hlf and Tef show accelerated ageing and premature death (21), and mice homozygous for Clock have altered diurnal feeding and a complex hyperphagic, hyperlipidaemic, hyperglycaemic, hypoinsulinaemic and obese phenotype (59). These findings, and our data, suggest circadian rhythm genes may be important in mammalian energy balance. While feeding

time *per se* does not impinge on lifespan-extension during CR (44), changes in circadian gene transcription following acute CR may be relevant to lifespan extension, as age-related impairments in sleep patterns are well established (48), alterations in circadian rhythm impinge negatively on lifespan in various organisms (5), and shift-work in humans is associated with elevated plasma glucose and lipid levels, a greater risk of cardiovascular disease, cancer, diabetes and overall mortality (33).

Mice undergoing acute CR rapidly adopt many transcriptional changes of long-term CR. Several hepatic EASE categories altered following long-term CR (16) were also seen in acute CR, including an up-regulation of categories involved in electron transport, mitochondria and fatty acid metabolism. Interestingly, several categories showed discordance between long-term and acute CR. The categories B-class cytochrome P450 and short-chain dehydrogenase/reductase were up-regulated during acute CR but down-regulated by long-term CR and appear important C. *elegans* longevity assurance (42).

Our cross-tissue comparison identified several potential longevity assurance genes (and pathways) altered in common across tissues. We suggest our simultaneous analysis of transcriptional and metabolite alterations is a powerful technique that may narrow down and help identify mechanisms through which CR extends lifespan, and that the benefits associated with CR may require only a short-term reduction in caloric intake.

ACKNOWLEDGMENTS

We thank Andrew Craig, Roger Tatoud and Olivier Cloarec for bioinformatic advice. We are grateful to Mike Hubank and Nipurna Jina at the Institute of Child Health Gene

Microarray Centre, University College London, U.K. for microarray and bioinformatics support.

GRANTS

This work was performed under the Functional Genomics of Ageing Consortium supported by the Wellcome Trust Functional Genomics Programme (to Dominic Withers, Linda Partridge, Janet Thornton, David Gems), Research into Ageing and The Rosetrees Trust (to Dominic Withers, Linda Partridge, David Gems), BBSRC and EMBL (to Janet Thornton).

REFERENCES

1. **Amador-Noguez D, Yagi K, Venable S, and Darlington G.** Gene expression profile of long-lived Ames dwarf mice and Little mice. *Aging Cell* 3: 423-441, 2004.
2. **Argentino DP, Dominici FP, Al-Regaiey K, Bonkowski MS, Bartke A, and Turyn D.** Effects of long-term caloric restriction on early steps of the insulin-signaling system in mouse skeletal muscle. *J Gerontol A Biol Sci Med Sci* 60: 28-34, 2005.
3. **Argentino DP, Dominici FP, Munoz MC, Al-Regaiey K, Bartke A, and Turyn D.** Effects of long-term caloric restriction on glucose homeostasis and on the first steps of the insulin signaling system in skeletal muscle of normal and Ames dwarf (Prop1df/Prop1df) mice. *Exp Gerontol* 40: 27-35, 2005.
4. **Argentino DP, Munoz MC, Rocha JS, Bartke A, Turyn D, and Dominici FP.** Short-term caloric restriction does not modify the in vivo insulin signaling pathway leading to Akt activation in skeletal muscle of Ames dwarf (Prop1(df)/Prop1(df)) mice. *Horm Metab Res* 37: 672-679, 2005.
5. **Aujard F, Dkhissi-Benyahya O, Fournier I, Claustrat B, Schilling A, Cooper HM, and Perret M.** Artificially accelerated aging by shortened photoperiod alters early gene expression (Fos) in the suprachiasmatic nucleus and sulfatoxymelatonin excretion in a small primate, Microcebus murinus. *Neuroscience* 105: 403-412, 2001.
6. **Badman MK and Flier JS.** The gut and energy balance: visceral allies in the obesity wars. *Science* 307: 1909-1914, 2005.
7. **Bartke A, Wright JC, Mattison JA, Ingram DK, Miller RA, and Roth GS.** Extending the lifespan of long-lived mice. *Nature* 414: 412, 2001.
8. **Bauer M, Hamm AC, Bonaus M, Jacob A, Jaekel J, Schorle H, Pankratz MJ, and Katzenberger JD.** Starvation response in mouse liver shows strong correlation with life-span-prolonging processes. *Physiol Genomics* 17: 230-244, 2004.
9. **Beckwith-Hall BM, Brindle JT, Barton RH, Coen M, Holmes E, Nicholson JK, and Antti H.** Application of orthogonal signal correction to minimise the effects of physical and biological variation in high resolution 1H NMR spectra of biofluids. *Analyst* 127: 1283-1288, 2002.
10. **Boylston WH, Gerstner A, DeFord JH, Madsen M, Flurkey K, Harrison DE, and Papaconstantinou J.** Altered cholesterologenic and lipogenic transcriptional profile in livers of aging Snell dwarf (Pit1dw/dwJ) mice. *Aging Cell* 3: 283-296, 2004.
11. **Cao SX, Dhahbi JM, Mote PL, and Spindler SR.** Genomic profiling of short- and long-term caloric restriction effects in the liver of aging mice. *Proc Natl Acad Sci U S A* 98: 10630-10635, 2001.
12. **Cartee GD and Dean DJ.** Glucose transport with brief dietary restriction: heterogenous responses in muscles. *Am J Physiol* 266: E946-952, 1994.
13. **Choe SE, Boutros M, Michelson AM, Church GM, and Halfon MS.** Preferred analysis methods for Affymetrix GeneChips revealed by a wholly defined control dataset. *Genome Biol* 6: R16, 2005.
14. **Choudhury AI, Heffron H, Smith MA, Al-Qassab H, Xu AW, Selman C, Simmgen M, Clements M, Claret M, Maccoll G, Bedford DC, Hisadome K, Diakonov I, Moosajee V, Bell JD, Speakman JR, Batterham RL, Barsh GS, Ashford ML, and Withers DJ.** The role of insulin receptor substrate 2 in hypothalamic and beta cell function. *J Clin Invest* 115: 940-950, 2005.

15. **Clancy DJ, Gems D, Harshman LG, Oldham S, Stocker H, Hafen E, Leevers SJ, and Partridge L.** Extension of life-span by loss of CHICO, a Drosophila insulin receptor substrate protein. *Science* 292: 104-106, 2001.
16. **Dhahbi JM, Kim HJ, Mote PL, Beaver RJ, and Spindler SR.** Temporal linkage between the phenotypic and genomic responses to caloric restriction. *Proc Natl Acad Sci U S A* 101: 5524-5529, 2004.
17. **Dominici FP, Hauck S, Argentino DP, Bartke A, and Turyn D.** Increased insulin sensitivity and upregulation of insulin receptor, insulin receptor substrate (IRS)-1 and IRS-2 in liver of Ames dwarf mice. *J Endocrinol* 173: 81-94, 2002.
18. **Fontana L, Meyer TE, Klein S, and Holloszy JO.** Long-term calorie restriction is highly effective in reducing the risk for atherosclerosis in humans. *Proc Natl Acad Sci U S A* 101: 6659-6663, 2004.
19. **Friedlander AL, Braun B, Pollack M, MacDonald JR, Fulco CS, Muza SR, Rock PB, Henderson GC, Horning MA, Brooks GA, Hoffman AR, and Cymerman A.** Three weeks of caloric restriction alters protein metabolism in normal-weight, young men. *Am J Physiol Endocrinol Metab* 289: E446-455, 2005.
20. **Fu C, Xi L, McCarter R, Hickey M, and Han ES.** Early hypothalamic response to age-dependent gene expression by calorie restriction. *Neurobiol Aging*, 2005.
21. **Gachon F, Fonjallaz P, Damiola F, Gos P, Kodama T, Zakany J, Duboule D, Petit B, Tafti M, and Schibler U.** The loss of circadian PAR bZip transcription factors results in epilepsy. *Genes Dev* 18: 1397-1412, 2004.
22. **Gazdag AC, Dumke CL, Kahn CR, and Cartee GD.** Calorie restriction increases insulin-stimulated glucose transport in skeletal muscle from IRS-1 knockout mice. *Diabetes* 48: 1930-1936, 1999.
23. **Giannakou ME, Goss M, Junger MA, Hafen E, Leevers SJ, and Partridge L.** Long-lived Drosophila with overexpressed dFOXO in adult fat body. *Science* 305: 361, 2004.
24. **Guarente L.** Calorie restriction and SIR2 genes--towards a mechanism. *Mech Ageing Dev* 126: 923-928, 2005.
25. **Hosack DA, Dennis G, Jr., Sherman BT, Lane HC, and Lempicki RA.** Identifying biological themes within lists of genes with EASE. *Genome Biol* 4: R70, 2003.
26. **Houthoofd K, Braeckman BP, Johnson TE, and Vanfleteren JR.** Life extension via dietary restriction is independent of the Ins/IGF-1 signalling pathway in Caenorhabditis elegans. *Exp Gerontol* 38: 947-954, 2003.
27. **Hwangbo DS, Gershman B, Tu MP, Palmer M, and Tatar M.** Drosophila dFOXO controls lifespan and regulates insulin signalling in brain and fat body. *Nature* 429: 562-566, 2004.
28. **Ikeno Y, Hubbard GB, Lee S, Richardson A, Strong R, Diaz V, and Nelson JF.** Housing density does not influence the longevity effect of calorie restriction. *J Gerontol A Biol Sci Med Sci* 60: 1510-1517, 2005.
29. **Kaput J, Klein KG, Reyes EJ, Kibbe WA, Cooney CA, Jovanovic B, Visek WJ, and Wolff GL.** Identification of genes contributing to the obese yellow Avy phenotype: caloric restriction, genotype, diet x genotype interactions. *Physiol Genomics* 18: 316-324, 2004.

30. **Kendziorski C, Irizarry RA, Chen KS, Haag JD, and Gould MN.** On the utility of pooling biological samples in microarray experiments. *Proc Natl Acad Sci U S A* 102: 4252-4257, 2005.
31. **Kendziorski CM, Zhang Y, Lan H, and Attie AD.** The efficiency of pooling mRNA in microarray experiments. *Biostatistics* 4: 465-477, 2003.
32. **Kenyon C.** The plasticity of aging: insights from long-lived mutants. *Cell* 120: 449-460, 2005.
33. **Knutsson A, Hammar N, and Karlsson B.** Shift workers' mortality scrutinized. *Chronobiol Int* 21: 1049-1053, 2004.
34. **Kobayashi Y, Furukawa-Hibi Y, Chen C, Horio Y, Isobe K, Ikeda K, and Motoyama N.** SIRT1 is critical regulator of FOXO-mediated transcription in response to oxidative stress. *Int J Mol Med* 16: 237-243, 2005.
35. **Lakowski B and Hekimi S.** The genetics of caloric restriction in Caenorhabditis elegans. *Proc Natl Acad Sci U S A* 95: 13091-13096, 1998.
36. **Lee CK, Klopp RG, Weindruch R, and Prolla TA.** Gene expression profile of aging and its retardation by caloric restriction. *Science* 285: 1390-1393, 1999.
37. **Liepa GU, Masoro EJ, Bertrand HA, and Yu BP.** Food restriction as a modulator of age-related changes in serum lipids. *Am J Physiol* 238: E253-257, 1980.
38. **Lin K, Hsin H, Libina N, and Kenyon C.** Regulation of the Caenorhabditis elegans longevity protein DAF-16 by insulin/IGF-1 and germline signaling. *Nat Genet* 28: 139-145, 2001.
39. **Liu G, Loraine AE, Shigeta R, Cline M, Cheng J, Valmeekam V, Sun S, Kulp D, and Siani-Rose MA.** NetAffx: Affymetrix probesets and annotations. *Nucleic Acids Res* 31: 82-86, 2003.
40. **Mair W, Goymer P, Pletcher SD, and Partridge L.** Demography of dietary restriction and death in Drosophila. *Science* 301: 1731-1733, 2003.
41. **Masoro EJ.** Overview of caloric restriction and ageing. *Mech Ageing Dev*, 2005.
42. **McElwee JJ, Schuster E, Blanc E, Thomas JH, and Gems D.** Shared transcriptional signature in Caenorhabditis elegans Dauer larvae and long-lived daf-2 mutants implicates detoxification system in longevity assurance. *J Biol Chem* 279: 44533-44543, 2004.
43. **Miller RA, Chang Y, Galecki AT, Al-Regaiey K, Kopchick JJ, and Bartke A.** Gene expression patterns in calorically restricted mice: partial overlap with long-lived mutant mice. *Mol Endocrinol* 16: 2657-2666, 2002.
44. **Nelson W.** Food restriction, circadian disorder and longevity of rats and mice. *J Nutr* 118: 286-289, 1988.
45. **Nisoli E, Tonello C, Cardile A, Cozzi V, Bracale R, Tedesco L, Falcone S, Valerio A, Cantoni O, Clementi E, Moncada S, and Carruba MO.** Calorie restriction promotes mitochondrial biogenesis by inducing the expression of eNOS. *Science* 310: 314-317, 2005.
46. **Partridge L, Piper MD, and Mair W.** Dietary restriction in Drosophila. *Mech Ageing Dev*, 2005.
47. **Pletcher SD, Macdonald SJ, Marguerie R, Certa U, Stearns SC, Goldstein DB, and Partridge L.** Genome-wide transcript profiles in aging and calorically restricted Drosophila melanogaster. *Curr Biol* 12: 712-723, 2002.

48. **Prinz PN.** Age impairments in sleep, metabolic and immune functions. *Exp Gerontol* 39: 1739-1743, 2004.
49. **Pugh TD, Oberley TD, and Weindruch R.** Dietary intervention at middle age: caloric restriction but not dehydroepiandrosterone sulfate increases lifespan and lifetime cancer incidence in mice. *Cancer Res* 59: 1642-1648, 1999.
50. **Puigserver P, Rhee J, Donovan J, Walkey CJ, Yoon JC, Oriente F, Kitamura Y, Altomonte J, Dong H, Accili D, and Spiegelman BM.** Insulin-regulated hepatic gluconeogenesis through FOXO1-PGC-1alpha interaction. *Nature* 423: 550-555, 2003.
51. **Raju J and Bird RP.** Energy restriction reduces the number of advanced aberrant crypt foci and attenuates the expression of colonic transforming growth factor beta and cyclooxygenase isoforms in Zucker obese (fa/fa) rats. *Cancer Res* 63: 6595-6601, 2003.
52. **Reiling JH and Hafen E.** The hypoxia-induced paralogs Scylla and Charybdis inhibit growth by down-regulating S6K activity upstream of TSC in Drosophila. *Genes Dev* 18: 2879-2892, 2004.
53. **Schibler U.** The daily rhythms of genes, cells and organs. *EMBO Rep* 6: S9-S13, 2005.
54. **Selman C, Phillips T, Staib JL, Duncan JS, Leeuwenburgh C, and Speakman JR.**Energy expenditure of calorically restricted rats is higher than predicted from their altered body composition. *Mech Ageing Dev* 126: 783-793, 2005.
55. **Sharp ZD and Bartke A.** Evidence for down-regulation of phosphoinositide 3-kinase/Akt/mammalian target of rapamycin (PI3K/Akt/mTOR)-dependent translation regulatory signaling pathways in Ames dwarf mice. *J Gerontol A Biol Sci Med Sci* 60: 293-300, 2005.
56. **Solanky KS, Bailey NJ, Beckwith-Hall BM, Bingham S, Davis A, Holmes E, Nicholson JK, and Cassidy A.** Biofluid 1H NMR-based metabonomic techniques in nutrition research - metabolic effects of dietary isoflavones in humans. *J Nutr Biochem* 16: 236-244, 2005.
57. **Spindler SR.** Calorie restriction enhances the expression of key metabolic enzymes associated with protein renewal during aging. *Ann N Y Acad Sci* 928: 296-304, 2001.
58. **Tsuchiya T, Dhahbi JM, Cui X, Mote PL, Bartke A, and Spindler SR.** Additive regulation of hepatic gene expression by dwarfism and caloric restriction. *Physiol Genomics* 17: 307-315, 2004.
59. **Turek FW, Joshu C, Kohsaka A, Lin E, Ivanova G, McDearmon E, Laposky A, Losee-Olson S, Easton A, Jensen DR, Eckel RH, Takahashi JS, and Bass J.** Obesity and metabolic syndrome in circadian Clock mutant mice. *Science* 308: 1043-1045, 2005.
60. **Um SH, Frigerio F, Watanabe M, Picard F, Joaquin M, Sticker M, Fumagalli S, Allegrini PR, Kozma SC, Auwerx J, and Thomas G.** Absence of S6K1 protects against age- and diet-induced obesity while enhancing insulin sensitivity. *Nature* 431: 200-205, 2004.
61. **Walker G, Houthoofd K, Vanfleteren JR, and Gems D.** Dietary restriction in C. elegans: from rate-of-living effects to nutrient sensing pathways. *Mech Ageing Dev* 126: 929-937, 2005.
62. **Withers DJ.** Insulin receptor substrate proteins and neuroendocrine function. *Biochem Soc Trans* 29: 525-529, 2001.

63. **Wold S, Esbensen K, and Geladi P.** Principal component analysis. *Chemometrics and Intelligent Laboratory Systems* 2: 37-52, 1987.
64. **Wold S, Sjöström M, and Eriksson L.** PLS-regression: A basic tool of chemometrics. *Chemometrics and Intelligent Laboratory Systems* 58: 109-130, 2001.

Table 1. Using a metabonomic approach and partial least squares discriminant analysis, we determined the plasma metabolite profile of mice used to examine transcription. The 13 metabolites which had the greatest impact on our model, using the principal components 1 and 3 are shown. The number of arrows denotes the impact and direction of change of a particular metabolite on our model, following acute CR relative to AD controls. These metabolites were also ranked by importance to the first component of the model only, using the variable influence on projection parameter (VIP), which provides a score of the importance of the variables on the model. A metabolite chemical shift was the difference between the resonance frequency of a nucleus within a molecule, relative to a laboratory standard used to identify it within the NMR spectra. VLDL - Very low density lipoprotein.

Euclidean Sum Components 1&3	VIP Score Component 1 only	Metabolite	Metabolite chemical shift (ppm)
↑↑↑↑↑	2.57	Lactate	1.33
↑↑	5.61	Cholesterol	0.84
↑	2.34	Creatine	3.04
↑	1.54	Methionine	2.13
↑	1.36	3-Hydroxybutyrate	2.31
↑	0.97	Glutamine	2.41
↑	0.88	Acetate	1.91
↑	0.85	Valine	1.02
↑	0.76	Alanine	1.46
↓	0.70	Glyceryl of Lipids	4.06
↓	3.86	Glucose	3.83, 3.90
↓↓-↓↓↓	8.18	Choline	3.21
↓↓ -↓↓↓↓	10.08	Lipid (mainly VLDL)	0.87, 1.25-1.29

Table 2. Main over-represented tissue-specific gene classes determined by EASE (P<0.05) in liver, muscle, colon and hypothalamus following acute CR relative to AD control mice. The number of unique genes per category is indicated in parentheses. For additional EASE categories refer to supplementary data.

Theme	Category	Hits List / Hits Chip
Liver down-regulated		
General metabolism (196)	Kegg pathway Metabolism	61/757
	GO:0009058 biosynthesis	42/590
	GO:0009059 macromolecule biosynthesis	31/399
	GO:0008152 metabolism	181/3923
Lipid / steroid metabolism (26)	GO:0006694 steroid biosynthesis	10/29
	GO:0008610 lipid biosynthesis	17/108
	GO:0008202 steroid metabolism	12/58
	GO:0016126 sterol biosynthesis	6/11
	GO:0016125 sterol metabolism	8/29
	GO:0006629 lipid metabolism	25/283
	IPR002225 3-beta hydroxysteroid dehydrogenase/isomerase	4/5
	Kegg pathway Biosynthesis of steroids	5/13
	GO:0008203 cholesterol metabolism	6/25
	GO:0006695 cholesterol biosynthesis	4/8
	GO:0003854 3-beta-hydroxy-delta5-steroid dehydrogenase activity	3/3
Amino acid / amine metabolism (29)	GO:0009308 amine metabolism	18/152
	GO:0006519 amino acid and derivative metabolism	17/139
	Kegg pathway Amino Acid Metabolism	23/203
	GO:0006520 amino acid metabolism	14/105
	Kegg pathway Glycine, serine and threonine metabolism	7/23
	Kegg pathway Tyrosine metabolism	7/31
	GO:0004645 phosphorylase activity	3/4
	IPR007743 Interferon-inducible GTPase	3/5
	IPR006163 Phosphopantetheine-binding	3/5
Liver up-regulated		
Lipid metabolism (47)	GO:0006629 lipid metabolism	34/283
	GO:0006631 fatty acid metabolism	14/83
	Kegg pathway Fatty acid metabolism	10/43
	GO:0016289 CoA hydrolase activity	5/9
	GO:0006641 triacylglycerol metabolism	6/16
	Kegg pathway Lipid Metabolism	19/162
	GO:0016290 palmitoyl-CoA hydrolase activity	4/6
	GO:0006637 acyl-CoA metabolism	4/6

	GO:0019752 carboxylic acid metabolism	22/221
Oxidoreductase activity (40)	GO:0016491 oxidoreductase activity	39/411
	IPR000759 Adrenodoxin reductase	6/23
	GO:0016616 oxidoreductase activity, acting on the CH-OH group of donors, NAD or NADP as acceptor	8/55
Mitochondrion (44)	GO:0005739 mitochondrion	41/464
	IPR002067 Mitochondrial carrier protein	7/41
	IPR001993 Mitochondrial substrate carrier	9/72
	IPR002113 Adenine nucleotide translocator 1	6/38
Esterase / lipase / thioesterase (14)	IPR000379 Esterase/lipase/thioesterase	13/92
	GO:0004759 serine esterase activity	6/14
Coenzyme and prosthetic group metabolism (14)	GO:0006732 coenzyme metabolism	13/88
	GO:0006731 coenzyme and prosthetic group metabolism	14/101
Amino acid metabolism (24)	Kegg pathway Amino Acid Metabolism	22/203
	Kegg pathway Metabolism of Other Amino Acids	8/51
Regulation of biosynthesis mostly protein biosynthesis (10)	GO:0009889 regulation of biosynthesis	10/68
	GO:0006445 regulation of translation	6/26
	GO:0006417 regulation of protein biosynthesis	9/66
Membrane fraction (22)	GO:0042598 vesicular fraction	9/59
	GO:0005792 microsome	8/56
	GO:0005624 membrane fraction	13/134
Skeletal muscle down-regulated		
Intracellular transport (10)	GO:0046907 intracellular transport	10/254
	GO:0006886 intracellular protein transport	8/77
	GO:0006605 protein targeting	5/70
Collagen (5)	IPR000885 Fibrillar collagen, C-terminal	3/7
	IPR008160 Collagen triple helix repeat	5/59
Macromolecule metabolism (32)	GO:0043170 macromolecule metabolism	32/1904
	GO:0009059 macromolecule biosynthesis	10/399
Protein metabolism (29)	GO:0019538 protein metabolism	28/1599
	Kegg ortholog Peptidylprolyl isomerase	3/18
	IPR000127 Ubiquitin-activating enzyme repeat	2/4
Skeletal muscle up-regulated		
Regulation of enzyme (mostly kinase) activity (5)	GO:0050790 regulation of enzyme activity	5/63
	GO:0045859 regulation of protein kinase activity	4/35
	GO:0006469 negative regulation of protein kinase activity	3/70
Carbohydrate metabolism (6)	Kegg pathway Glycolysis/Gluconeogenesis	4/42
	Kegg pathway Carbohydrate metabolism	6/191
Lipid / fatty acid metabolism (10)	GO:0006631 fatty acid metabolism	5/83
	GO:0019752 carboxylic acid metabolism	7/221
	GO:0006629 lipid metabolism	8/283
	GO:0016291 acyl-CoA thioesterase activity	2/68
Energy metabolism	Kegg pathway Energy metabolism	6/136

(6)	Kegg pathway Carbon fixation	3/17
MAPK signalling related (3)	GO:0007254 JNK cascade	3/19
	GO:0000186 activation of MAPKK	2/2
Clon down -regulated		
Cell growth and / or maintenance (30)	GO:0008151 cell growth/maintenance	30/1995
	GO:0000793 condensed chromosome	4/27
	GO:0005694 chromosome	6/124
	GO:0006259 DNA metabolism	7/272
Cell proliferation, part of cell growth / maintenance (22)	GO:0008283 cell proliferation	22/484
	GO:0007049 cell cycle	19/365
	Kegg pathway Cell cycle	3/19
	GO:0007067 mitosis	11/65
	GO:0000796 condensin complex	2/2
	GO:0000067 DNA replication and chromosome cycle	8/95
	GO:0006261 DNA-dependent DNA replication	4/30
	GO:0006270 DNA replication initiation	3/8
	GO:0006260 DNA replication	5/74
Purine nucleotide binding (16)	GO:0005524 ATP binding	15/737
	GO:0017076 purine nucleotide binding	16/944
Protein kinase (9)	IPR002290 Serine/threonine protein kinase	8/238
	GO:0004672 protein kinase activity	8/349
Colon up-regulated		
Rhythmic behaviour / circadian rhythm (5)	GO:0007622 rhythmic behavior	5/20
	GO:0007623 circadian rhythm	3/14
Transport /ion transport (10)	GO:0006814 sodium ion transport	5/44
	GO:0008509 anion transporter activity	4/29
	GO:0006811 ion transport	9/417
	GO:0006820 anion transport	5/121
	GO:0015075 ion transporter activity	5/148
	GO:0015291 porter activity	5/117
	GO:0005386 carrier activity	6/220
Membrane located (25)	GO:0016021 integral to membrane	22/2295
	GO:0016020 membrane	25/2886
Nitric oxide Mediated signal transduction and zinc ion homeostasis (2)	GO:0007263 nitric oxide mediated signal transduction	2/2
	GO:0006882 zinc ion homeostasis	2/2
Hypothalamus down-regulated		
Development (11)	GO:0007275 development	11/1066
	GO:0009653 morphogenesis	8/671
	GO:0009887 organogenesis	6/567
Other	GO:0005488 binding	25/4736
	GO:0005515 protein binding	13/1621
	GO:0050794 regulation of cellular process	6/430
	IPR000867 Insulin-like growth factor-binding protein, IGFBP	2/12

Hypothalamus up-regulated		
Other	GO:0009755 hormone-mediated signalling	2/6
	GO:0005488 binding	15/4736
	IPR000306 Zn-finger, FYVE type	2/23
	GO:0005604 basement membrane	2/24

Table 3. Main over-represented EASE categories (P<0.1) in the up-regulated gene list when comparing across tissues following acute CR.

Category	Category up in > 1 tissue	Tissues
Transporter activity	GO:0005215 transporter activity	colon, liver
	GO:0015291 porter activity	colon, liver
	GO:0005386 carrier activity	colon, liver
	GO:0015075 ion transporter activity	colon, liver
Ion homeostasis	GO:0019725 cell homeostasis	colon, liver
	GO:0006873 cell ion homeostasis	colon, liver
	GO:0046916 transition metal ion homeostasis	colon, liver
Zinc ion homeostasis /nitric oxide mediated signal transduction		
	GO:0006882 zinc ion homeostasis	colon, liver
	GO:0007263 nitric oxide mediated signal transduction	colon, liver
Aminotransferase	IPR001176 1-aminocyclopropane-1-carboxylate synthase	colon, liver
	IPR004839 Aminotransferase, class I and II	colon, liver
Other	GO:0016788 hydrolase activity, acting on ester bonds	colon, liver
	GO:0007622 rhythmic behaviour	colon, liver
	GO:0016020 membrane	colon, liver
Lipid metabolism	GO:0006637 acyl-CoA metabolism	liver, muscle
	GO:0016790 thiolester hydrolase activity	liver, muscle
	GO:0016291 acyl-CoA thioesterase activity	liver, muscle
	GO:0016290 palmitoyl-CoA hydrolase activity	liver, muscle
	GO:0016289 CoA hydrolase activity	liver, muscle
	GO:0006631 fatty acid metabolism	liver, muscle
Membrane located	GO:0005624 membrane fraction	liver, muscle
	GO:0042598 vesicular fraction	liver, muscle
Other	GO:0050790 regulation of enzyme activity	liver, muscle
	GO:0005829 cytosol	liver, muscle
	GO:0006800 oxygen and reactive oxygen species metabolism	liver, muscle
Other	GO:0005623 cell	colon, muscle

Table 4. Independent validation by real-time PCR of five genes significantly altered in the liver by acute CR and identified by our microarray analysis (pooled real-time PCR). Fold-changes refer to the ratio of the expression values of CR mice relative to AD mice. Statistical significance was calculated on normalized C_T values. In addition, real-time PCR of the same genes was run on liver RNA from each of the 20 individual mice (AD1:10, CR1:10) from which we derived our RNA pools (unpooled real-time PCR). Good agreement, in terms of fold-change and direction of change, was seen between the pooled and unpooled real-time PCR data and Affymetrix data. *Cyber-T test method generates Q values directly without producing P values.

	Pooled real-time PCR		**Affymetrix**		**Unpooled real-time PCR**	
Gene	Fold-change	P value	Fold-change	*Q value	Fold-change	P value
Insulin receptor substrate 1 (Irs1)	0.536	=0.05	0.646	<0.05	0.696	<0.05
Forkhead transcription factor 1 (Foxo1)	1.643	<0.05	1.936	<0.05	1.956	<0.0001
Peroxisome proliferator activated receptor alpha (Ppara)	1.645	<0.05	1.944	<0.01	1.549	<0.01
DNA-damage-inducible transcript 4 (Ddit4)	5.398	<0.01	5.951	<0.001	2.939	<0.01
Diacylglycerol O-acyltransferase 2 (Dgat2)	1.783	<0.01	1.443	<0.05	1.306	=0.11

FIGURE LEGEND

Figure 1. Partial least squares-discriminant analysis (PLS-DA) of plasma samples. Initial principal component analysis (PCA) separated plasma samples according to class (*ad libitum* (AD) and acute caloric restriction (CR)), so PLS-DA was used to maximize this separation and identify differences in metabolites (chemical shifts) that are the basis of this class separation. The scores scatter plot (a) illustrates that the CR replicates (red) were well-resolved from the AD replicates (black). The major variables responsible for class separation are revealed by the PLS-DA loadings scatter plot (b). This represents the chemical shift regions important to the inter-group differences within the discriminating model, and the relative magnitude of these differences in plasma metabolites between the two experimental groups. The metabolites responsible for the separation of classes are summarized in Table 1. Group separation was primarily explained by principal component 1 (PC1), whilst PC3 explained primarily within-group variation, especially within the CR group. PC2 also showed class separation, but is not reported as it was based solely on differences in lactate between groups.

Figure 2. Main tissue-specific EASE categories. Overview of the main tissue-specific EASE categories altered following acute CR. Up-regulated gene classes indicated in red and down-regulated genes in black. Note that the organs depicted are human for ease of recognition. No implication is made about the validity of these results in humans.

Figure 3. Number of shared genes up- and down-regulated across tissues. Comparative tissue response to acute caloric restriction. Up-regulated genes indicated in red and down-regulated genes in black. Significant relationships determined by overlaps in probe set lists across tissues using Fisher's Exact Probability Test. Number denotes

amount of genes shared between tissues. P<0.001 denoted by stippled line. P<0.0001 denoted by solid line.

Figure 4. Comparison of EASE categories generated from long- and acute CR. The number of significant (P<0.1) shared and unique hepatic EASE categories generated from the up-regulated and down-regulated gene lists from acute CR (this study) and long-term CR (16). Up-regulated EASE classes are shown in red and down-regulated EASE categories in black.

Figure 5. Global summary of metabolite and transcript changes following acute CR in mice. Main tissue-specific EASE categories reported for liver, muscle, hypothalamus and colon with arrows denoting up- (↑) or down-regulation (↓) in acute CR mice relative to AD controls. Plasma metabolites are identified in blue, with arrows, as above, denoting direction of change. EASE category overlap across tissues is identified by italics. We suggest acute CR, a period of negative energy balance, results in a hypothalamic drive for increased food intake and enhanced energy assimilation in the gastrointestinal tract. Plasma glucose and several plasma lipids decrease while transcripts involved in glucose metabolism, glucose transport and insulin sensitivity alter simultaneously across several tissues, and there is a marked decrease in hepatic lipid biosynthesis. We propose that white adipose tissue catabolism elevates plasma cholesterol, and there is increased liver and muscle β-oxidation, with metabolism rapidly switching from glycolysis towards lipolysis. Ketones, such as plasma 3-Hydroxybutyrate, are indicative of enhanced β-oxidation and can be utilized as an alternative energy source when glucose is limited, as during acute CR. However, we suggest that fat stores are depleted rapidly at this time, ultimately leading to a switch to gluconeogenesis as the primary energy generating

pathway. Muscle (and possibly colon) breakdown provides amino acid precursors for gluconeogenesis, with elevated plasma glutamine also helping to maintain acid-base balance, thus avoiding ketoacidosis. Elevated lactate suggests partial metabolism of glucose during acute CR thereby returning C_3 compounds (e.g. lactate) to the liver for gluconeogenesis. Note that the organs depicted are human for ease of recognition. No implication is made about the validity of these results in humans.

Figure 1.

a)

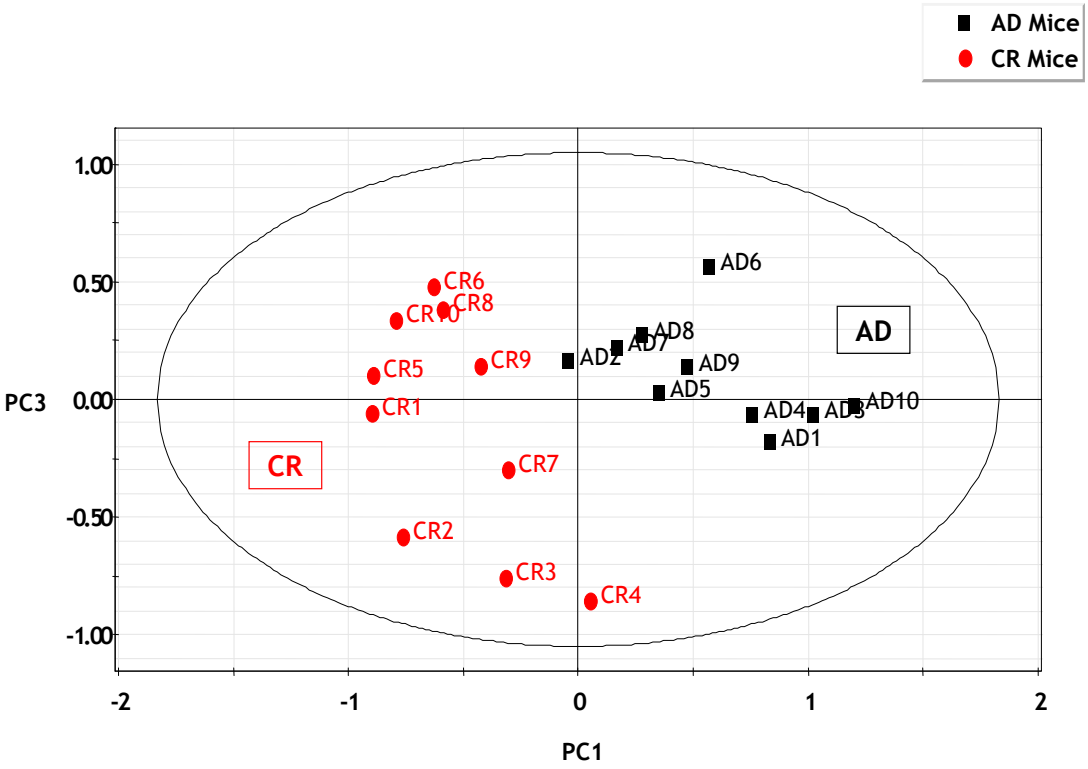
AD Mice
CR Mice
1.00
0.50
0.00
-0.50
-1.00
PC3
-2
-1
0
1
2
PC1
AD
CR
CR6
CR8
CR10
CR5
CR9
CR1
CR7
CR2
CR3
CR4
AD6
AD8
AD7
AD2
AD9
AD5
AD4
AD3
AD10
AD1

Figure 1

b)

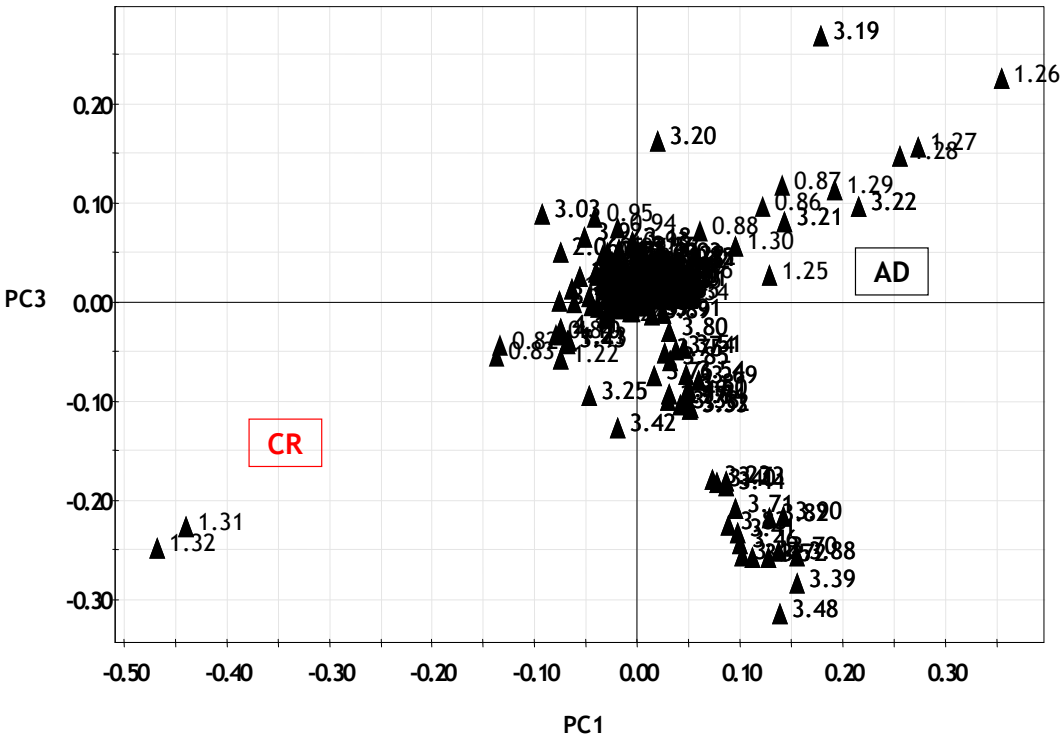
3.19
1.26
3.20
1.27
1.28
0.87
1.29
3.03
0.95
0.86
3.22
3.21
0.88
1.30
1.25
AD
3.80
0.85
1.22
3.25
3.42
CR
1.31
1.32
3.39
3.48
0.20
0.10
0.00
-0.10
-0.20
-0.30
PC3
-0.50
-0.40
-0.30
-0.20
-0.10
0.00
0.10
0.20
0.30
PC1

Figure 2.

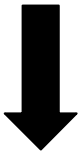

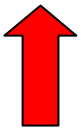

Development
- Morphogenesis
- Organogenesis

Binding
- Protein binding
- Regulation of cellular process

Hypothalamus

Hormone-mediated signalling
Binding
Basement membrane

General metabolism
- Macromolecule biosynthesis

Lipid/steroid metabolism
- Steroid biosynthesis
- Lipid biosynthesis
- Steroid metabolism
- Sterol biosynthesis

Amino acid/amine metabolism

Liver

Lipid metabolism
- Fatty acid metabolism
- CoA hydrolase activity
- Triacylglycerol metabolism

Oxidoreductase activity
Mitochondrion
Esterase/lipase/thioesterase
Coenzyme metabolism
Amino acid metabolism
Regulation of biosynthesis

Cell growth/maintenance
- Cell proliferation

Purine nucleotide binding
Protein kinase

Colon

Rhythmic behaviour
- Circadian rhythm

Transport/ion transport
Membrane located

Intracellular transport
- Protein transport
- Protein targeting

Collagen
Macromolecule metabolism
- Macromolecule biosynthesis

Protein metabolism

Muscle

Regulation of enzyme activity
Carbohydrate metabolism
- Lipid metabolism
- Fatty acid metabolism
- Carboxylic acid metabolism

Energy metabolism
MAPK signalling related

Figure 3.

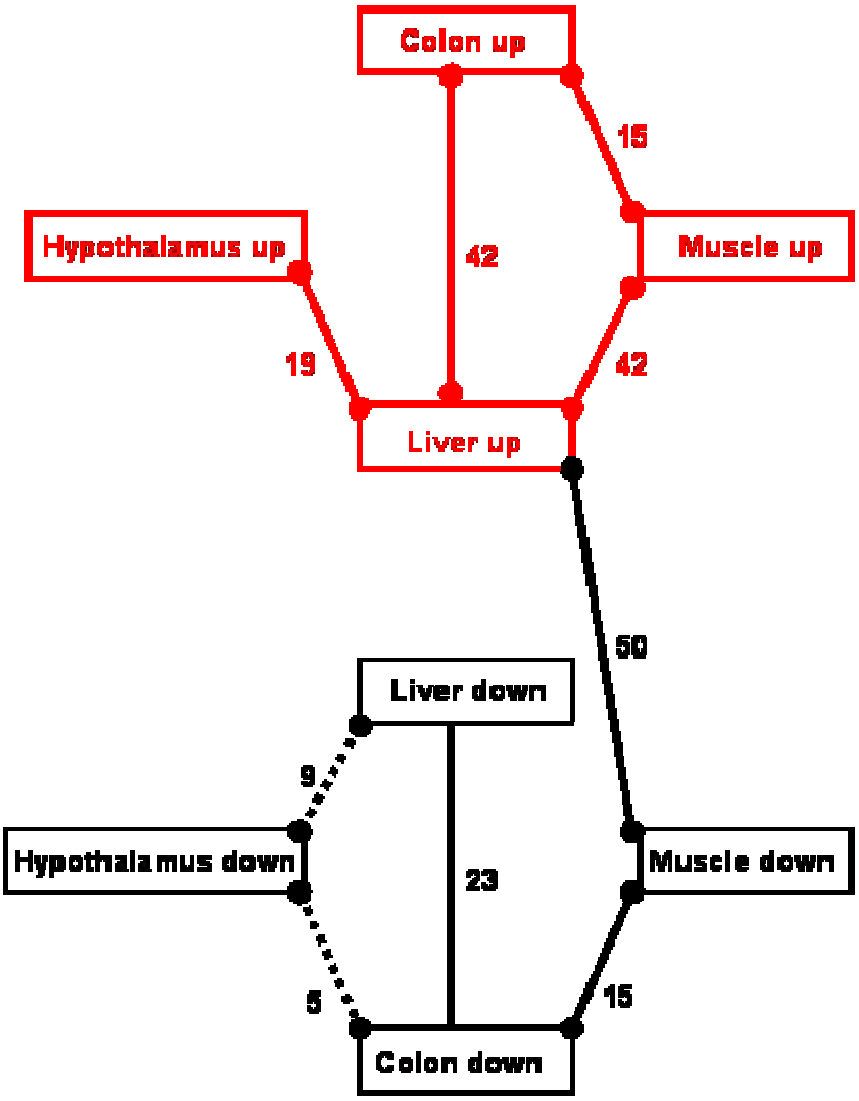
Colon up
15
Hypothalamus up
42
Muscle up
19
42
Liver up
50
Liver down
9
Hypothalamus down
23
Muscle down
5
15
Colon down

Figure 4.

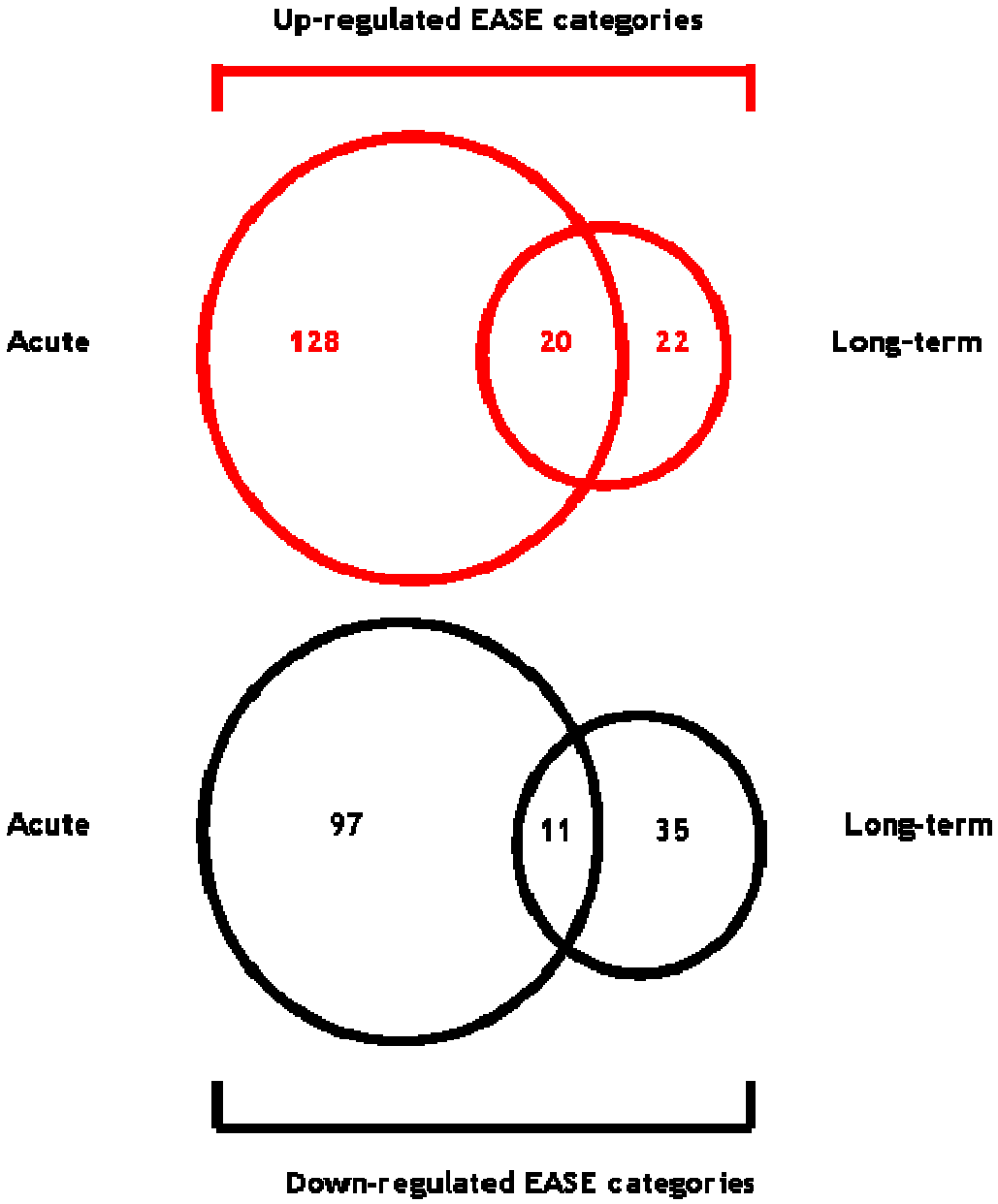
Up-regulated EASE categories
Acute
128
20
22
Long-term
Acute
97
11
35
Long-term
Down-regulated EASE categories

Figure 5.

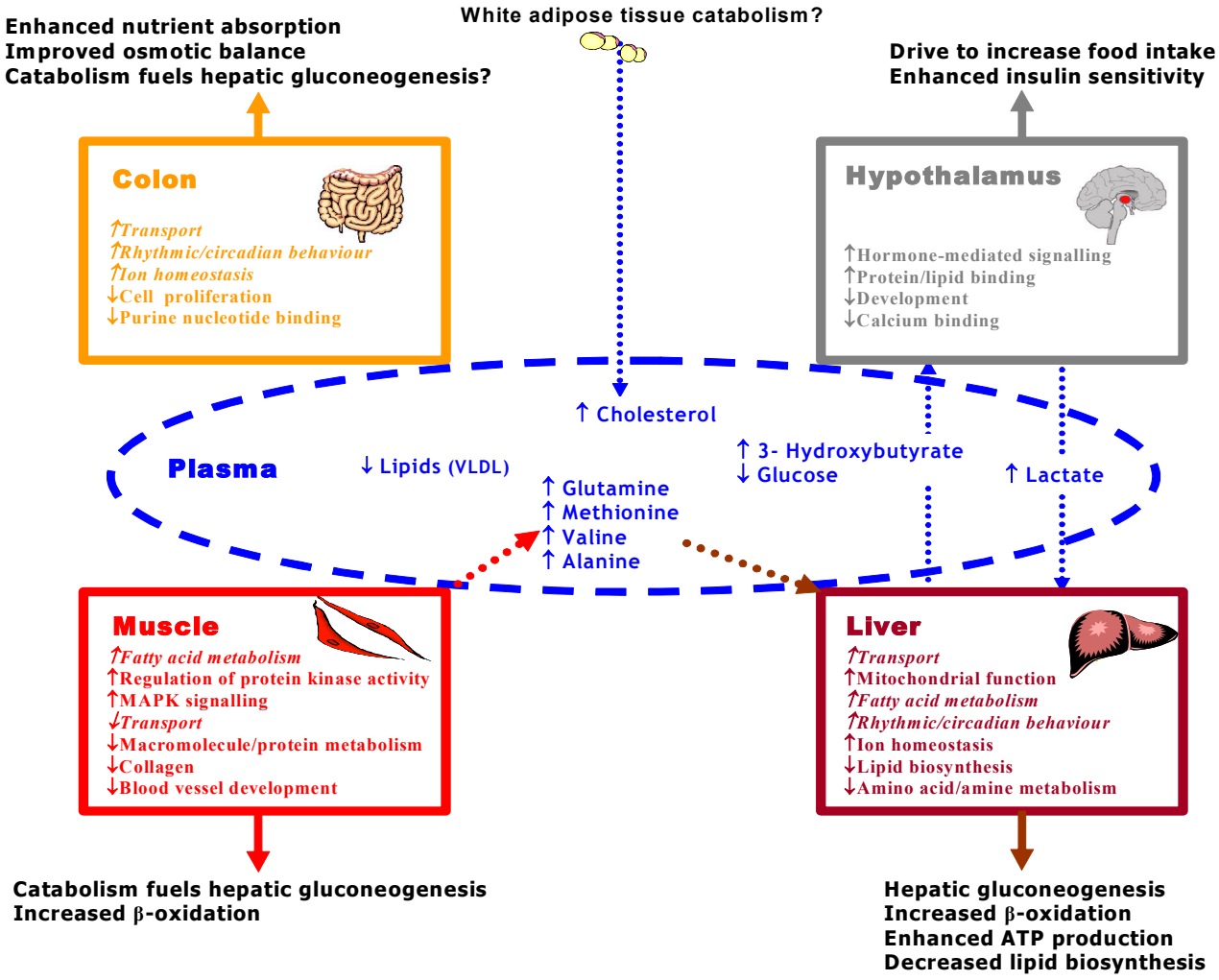
Enhanced nutrient absorption
Improved osmotic balance
Catabolism fuels hepatic gluconeogenesis?
White adipose tissue catabolism?
Drive to increase food intake
Enhanced insulin sensitivity
Colon
↑Transport
↑Rhythmic/circadian behaviour
↑Ion homeostasis
↓Cell proliferation
↓Purine nucleotide binding
Hypothalamus
↑Hormone-mediated signalling
↑Protein/lipid binding
↓Development
↓Calcium binding
↑ Cholesterol
Plasma
↓ Lipids (VLDL)
↑ 3- Hydroxybutyrate
↓ Glucose
↑ Lactate
↑ Glutamine
↑ Methionine
↑ Valine
↑ Alanine
Muscle
↑Fatty acid metabolism
↑Regulation of protein kinase activity
↑MAPK signalling
↓Transport
↓Macromolecule/protein metabolism
↓Collagen
↓Blood vessel development
Liver
↑Transport
↑Mitochondrial function
↑Fatty acid metabolism
↑Rhythmic/circadian behaviour
↑Ion homeostasis
↓Lipid biosynthesis
↓Amino acid/amine metabolism
Catabolism fuels hepatic gluconeogenesis
Increased β-oxidation
Hepatic gluconeogenesis
Increased β-oxidation
Enhanced ATP production
Decreased lipid biosynthesis